frontiers | Frontiers in Materials

TYPE Original Research
PUBLISHED 23 February 2023
DOI 10.3389/fmats.2023.1148589

OPEN ACCESS

EDITED BY
Pshtiwan Shakor,
Institute of Construction Materials, Australia

REVIEWED BY
Babar Ali,
COMSATS University Islamabad, Pakistan
Ahmed Salih Mohammed,
The American University of Iraq—Sulaimani, Iraq

*CORRESPONDENCE
Shaker Mahmood,
shaker730@yahoo.com

SPECIALTY SECTION
This article was submitted to Structural Materials, a section of the journal Frontiers in Materials

RECEIVED 20 January 2023
ACCEPTED 07 February 2023
PUBLISHED 23 February 2023

CITATION
Abed S, Hadi R, Jawdhari A, Mohammed Najm H, Mahmood S, Bilema M and Muayad Sabri Sabri M (2023), Influence of ternary hybrid fibers on the mechanical properties of ultrahigh-strength concrete. *Front. Mater.* 10:1148589. doi: 10.3389/fmats.2023.1148589

Influence of ternary hybrid fibers on the mechanical properties of ultrahigh-strength concrete

Suhad Abed[1], Rafal Hadi[2], Akram Jawdhari[3], Hadee Mohammed Najm[4], Shaker Mahmood[5,6]*, Munder Bilema[7] and Mohanad Muayad Sabri Sabri[8]

[1]Department of Highways and Airports Engineering, College of Engineering, University of Diyala, Diyala, Iraq, [2]Department of Civil Engineering, Bilad Alrafidain University College, Diyala, Iraq, [3]Department of Mechanical and Civil Engineering, Purdue University- Northwest, Hammond, IN, United States, [4]Department of Civil Engineering, Zakir Husain Engineering College, Aligarh Muslim University, Aligarh, India, [5]Department of Civil Engineering, College of Engineering, University of Duhok, Duhok, Iraq, [6]Department of Civil Engineering, College of Engineering, Nawroz University, Duhok, Iraq, [7]Department of Civil Technology, College of Science Technology- Qaminis, Qaminis, Libya, [8]Peter the Great St. Petersburg Polytechnic University, St Petersburg, Russia

Ultra-high performance concrete (UHPC), an advanced class of fiber-reinforced cementitious material with extraordinary mechanical properties, low permeability, shrinkage and creep, and high energy absorption capacity, has seen steady increase in use, with applications covering construction of new members and retrofit of existing ones. Fibers are added in the UHPC mix to bridge cracks, carry tensile stresses, and contribute greatly to member ductility and load capacity. Hybrid fibers comprising micro and macro types are beneficial where the first type resists microcracking and the second targets macrocracking. This study investigates the effects of blending three fiber types, namely, hooked-end steel (referred to as type 1, representing macro fibers class), straight-end steel (type 2, intermediate size fibers), and carbon (type 2, micro size fiber), on the mechanical properties of UHPC. Experimental tests were performed to characterize the following mechanical properties: flowability, compressive strength, tensile strength, flexural strength, modulus of elasticity, and dry shrinkage. The primary variable in the tests was the blending of different fiber types, using either a unary form of type 1, a binary form of type 1 and 3 or type 2 and 3, and a ternary mix of all three types, at 1.56% dosage by volume. The mix with ternary fibers yielded a compressive strength, tensile strength, flexural strength, and modulus of elasticity that is 14%–17%, 14%–16.8%, 43.66%–22.16%, and 12%–16%, larger than the same respective properties of the mix with unary fibers. In addition, ternary fibers increased the cohesiveness of the mix by 17% and 26% compared to unary fibers.

KEYWORDS

UHPC, fiber-reinforced concrete, reactive powder concrete, fibers, fiber reinforced polymer

1 Introduction

Ultra-high performance concrete (UHPC), also known as reactive powder concrete (RPC) and ultra-high performance fiber-reinforced concrete (UHPFRC) (Ter Maten, 2011; Qaidi et al., 2022a; Tayeh et al., 2022c), is an advanced class of fiber-reinforced cementitious material obtained through the removal of coarse aggregate, optimization of particle

gradation, use of admixtures and microfibers (Ter Maten, 2011; Saeed et al., 2022; Zeybek et al., 2022). It consists of fine powders such as cement, quartz, fine sand, and mineral additives such as fly ash, silica fume, and ground granulated blast-furnace slag, used due to their pozzolanic properties and filling capacity (Shakor et al., 2019a; Puzatova et al., 2022; Vinod et al., 2022). With a low w/c ratio [typically less than 0.25 (Graybeal, 2014; Sanjuán and Andrade, 2021)], superplasticizers are also used to ensure good flow, consolidation, and workability of UHPC (Caluk et al., 2019; Tayeh et al., 2022a; Qaidi et al., 2022f). Discontinuous fiber reinforcement, typically made from steel with diameters of 0.5 mm, lengths of 12.5 mm, and dosage of 2%–4% by volume, are incorporated in UHPC mix to provide bond at the micro level and minimize micro-cracking (Harris and Roberts-Wollmann, 2005). The mechanical properties of UHPC include a compressive strength (f_c') of more than 150 MPa, and tensile strength exceeding 5 MPa with a strain-hardening response resembling metallic ductility. UHPC has low permeability, shrinkage, and creep; good durability, and high energy absorption capacity.

While the high initial cost prohibits its application in mass construction, UHPC has been used mainly in applications that maximize its attributes, including in members subjected to harsh environments, as a repair overlay for bridge decks and corroded steel girders ends; in construction of link slabs, hybrid members containing UHPC in highly stressed regions such as beam mid-spans and column plastic hinges; and as grout material for joints between adjacent precast girders or between a precast slab and steel girder (Grünewald, 2004; Qaidi et al., 2022f; He et al., 2022). Nonetheless, with the development of open-source mixes which help to reduce the unit price, establishment of design codes and guidelines, abundance of research studies and filed applications, and presence of educational programs introducing various design and construction aspects to professional engineers and contractors, UHPC is becoming increasingly used in the construction of full members such as beams (Standard, 2017; Qaidi S. M. et al., 2022; Tayeh et al., 2022d; Qaidi et al., 2022f), thin shells (Ter Maten, 2011; Shakor et al., 2019b), concrete sandwich panels (Qaidi et al., 2022c), marine structures, piers, and sewage treatment units (Tayeh et al., 2022b; Qaidi et al., 2022c; Qaidi et al., 2022d; Qaidi et al., 2022e; Faraj et al., 2022; He et al., 2022).

Fibers have a crucial role within UHPC, mainly acting as stitches, bridging cracks and transferring load across their faces, thus increasing the member's ductility and load capacity (Emad et al., 2022; Faraj et al., 2022). Some of UHPC mechanical properties, particularly the post-cracking tensile stress-strain response, are dependent on fiber properties such as type, content, aspect ratio (length/diameter), combined stiffness (for fiber cocktail), and method of placement during casting (Ter Maten, 2011; Qaidi et al., 2021a; Almeshal et al., 2022). Multiple studies investigated key parameters related to the use of single-type fibers in UHPC. For example, Biolzi et al. (1997) studied the effects of three contents for steel fibers, namely: 2%, 4%, and 6% by volume, on UHPC's compressive strength, direct tensile strength, and elastic modulus. Gao (2007) compared the dynamic load performance of plain and fiber-reinforced UHPC (Ali et al., 2022a; Ali et al., 2022b).

While single-type fibers are predominantly used, multiple studies have found that using a mixture of fiber lengths and types, results in better ductility and strength. Fiber cocktails enable better-cracking resistance where short fibers act to bridge microcracks while long ones restrain macrocracks. Different fiber types have been found to result in different attributes, namely, a) steel fibers to increase fracture energy and strength, b) Polypropylene (PP) fibers to increase fire resistance and reduce spalling and early shrinkage, and c) glass fibers to reduce internal stresses in fresh UPHC. The study by Rossi et al. (1987) was one of the first to propose the mix of multi-type fibers with the product dubbed multi-modal fiber-reinforced concrete. Few studies investigated the effects of blending multi-type fibers in UHPC. Raza et al. (2021) examined three types of single fiber-reinforced UHPC, namely: steel fiber (SF), glass fiber (GF), and carbon fiber (CF), and three blended fiber mixes, namely: SF-GF, GF-CF, and CFSF. A constant volume fraction of 2% was used for all fiber combinations. The study concluded that using a hybrid mix of 1% SF and 1% CF yielded the maximum overall mechanical performance among all combinations. Shaheen and Shrive (2006) compared CF- and SF-reinforced UHPC and found the former to result in significantly higher fracture toughness, and compressive and splitting tensile strength than the latter (Cao et al., 2018b; Khan et al., 2018; Ahmad et al., 2020).

Despite the limited studies, there is a need to examine further the effects of multi-type and blended fibers on the behavior of UHPC (Cao et al., 2018a; Khan et al., 2021; Khan et al., 2022). This study aims to examine whether higher mechanical and durability properties in UHPC can be obtained if a blend of multiple fiber types representing a range of micro and macro types with different dimensions, end conditions, and textures are used instead of single fiber type. Three types of fibers were used in the study: hooked-end steel fibers as macro class, straight-end steel fibers as intermediate class, and carbon fibers as micro reinforcement. Experimental tests were performed to characterize the common mechanical properties: flowability, compressive strength, tensile strength, flexural strength, modulus of elasticity, and dry shrinkage.

2 Experimental work

To understand the effects of blended micro and macro fiber bundles on the behavior of UHPC, five mixes were chosen and tested comprising diverse types of fibers (carbon fibers and straight steel fibers as microfiber and steel fiber with hooked-ends as macro fiber) (Figure 1) in its single and hybrid states with different volumetric percentages (V_f). The properties of the fibers used are presented in Table 1. They include a) hooked-end steel fibers (after this referred to as type 1) with a length (L) and diameter (D) of 50 and 0.75 mm, respectively, representing the macro reinforcement; b) straight-end steel fibers (after this referred to as type 2) with L and D of 15 and 0.2 mm, respectively, as an intermediate size micro reinforcement; and carbon fibers (after this referred to as type 3) with L and D of 8 and 0.007 mm, as a smaller size micro reinforcement. The volume fraction of steel fibers used in this study was 1.33% depending on the published earlier study (Ahmed and Abd, 2018; Al-Tayeb et al., 2022; Akeed et al., 2022c; Emad et al., 2022; Faraj et al., 2022), while the carbon fiber ratio chosen was based on a general review of the literature.

The UHPC was produced using exceptionally fine materials including ordinary Portland cement (type I), river silica sand, and

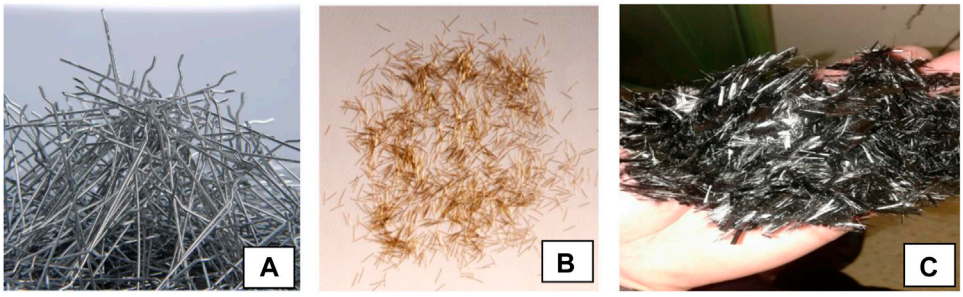

FIGURE 1
(A) Steel fibers with hooked ends, **(B)** steel fibers with straight ends, and **(C)** carbon fibers.

TABLE 1 Fiber properties.

Type of fibers	Steel fibers (hooked-ends)	Steel fibers (straight ends)	Carbon fibers
Length (mm)	50	15–16	8
Diameter (mm)	0.75	0.2 ± 0.02	7 ± 2 microns
Density (kg/m^3)	7,800	7,800	1,700
Aspect ratio (L/D)	50	40–80	1,140
Tensile strength (MPa)	1,345	2,000	3,500

silica fume, in addition to the use of a chemical additive superplasticizer (Gleinum 51) to reduce the w/c ratio to 20%. All the properties of the materials used are shown in Table 2, the sieve analysis of silica sand is shown in Table 3, and the details of the proportions of the mixture materials are shown in Table 4. Mixes 1 and 2 contain 1.33% of uni-type fibers, the former with type 1 and the latter with type 2, Table 4. Mix 3 contains a blend, of 1.33% of type 1% and 0.2% of type 3 fibers. Mix 4 features 1.33% of type 2 fibers and 0.2% of type 3, while mix 5 has a combination of 0.66% of type 1, 0.66% of type 2, and 0.2% of type 3 fibers. The effects of the hybrid fibers were characterized through material tests on several mechanical properties: compressive strength, tensile strength, flexural strength, and modulus of elasticity. Table 5 summarizes the various characterization tests performed on the mixes, showing the specimen configuration and dimensions for each test, along with the standard followed in each test.

To ensure that the fine particles overlap with each other and blend properly, the dry materials (cement, silica sand, and silica fume) were mixed for 3 min in a small rotary mixer. The superplasticizer was then diluted with the required water quantity and the final solution was added to the dry ingredients, where mixing was then continued for additional 2 min to obtain a homogeneous mixture. Finally, the fibers were distributed uniformly and gradually to prevent them from balling and agglomeration, while maintaining a uniform distribution over the mixture during the mixing period.

Before pouring the UHPC mix, the molds for material tests (i.e., cylinders, cubes, and prisms) were prepared by coating their inner surfaces with a thin layer of oil to facilitate specimen removal after the concrete hardens. The specimens were lightly tapped by a metal rod to reduce air voids and ensure good compaction. Figure 2 shows a representative sample of the freshly cast specimens in molds. The specimens were levelled using a trowel and then left to cure for 24 h. They were removed from the models and placed in a curing basin filled with water (Figure 3) until the required tests were performed at 7 and 28 days. A total of 90 specimens with different shapes (i.e., cubes, cylinders, and prisms) were prepared and tested for the 5 mixes in Table 4, at the ages of 7 and 28 days.

3 Experimental tests

3.1 Flow table test

A flow test, following ASTM C-1437 (ASTM, 2007) standards, was conducted (Figure 4) to measure the workability of the five UHPC mixes used in the study. The flow is defined as the average increase in the base diameter, measured at least in four different diameters at approximately equidistant intervals, and is expressed as a percentage of the original base diameter.

$$Flow = \left[\frac{D_{avg} - D_o}{D_o}\right] * 100$$

Where:

D_{avg} = Average base diameter measured after the mold is lifted and the mortar spreads.
D_o = Original base diameter of the mold.

TABLE 2 Material properties used in the current study.

Properties		Cement	Iraqi specification No. 5/1984	Silica sand	Silica fume	Superplasticizer
Form		Powder	—	Fine granules	Powder	Viscous liquid
Color		Dark gray	—	Light brown	Light gray	Light brown
Relative density		1,440 kg/m^2	—	1,600	—	1.1 @ 20 Co
pH		—	—	—	—	6.6
Viscosity		—	—	—	—	128 ± 30 CPS@ 20 Co
Specific gravity		—	—	2.63	—	—
Surface area m^2/kg		405	Minimum (230)	—	24,000-28,000	—
SiO_2	% (weight)	21.44	—	—	≥90	—
SO_3		2.7	Maximum (2.8)	—	≤0.2	—
CaO		61.19	—	—	≤0.8	—
C3A		5.73	—	—	—	—
C3S		42.83	—	—	—	—
C2S		29.4	—	—	—	—
C4AF		11.19	—	—	—	—
Sitting time: Initial (min.) Final (hr.)		135 3:25	Minimum (45) Maximum (10)	—	—	—
Compressive strength (MPa): 3- days 7- days		24.4 32.3	Minimum (15) Minimum (23)	—	—	—

TABLE 3 Sieve analysis of silica sand.

Sieve size	Passing %
600 μm	93
300 μm	23
150 μm	4.5
Pan	0

3.2 Compressive strength test

Compression tests were conducted according to BS 1881 (BS, 1989) on cubes with a side length of 100 mm using a hydraulic testing machine with a capacity of 2,000 kN, at a loading rate of 0.25 ± 0.05 MPa per second, as shown in Figure 5.

3.3 Splitting tensile strength test

Splitting tensile tests were performed according to ASTM C496 (Standard, 2017), on cylinders with diameters (D) and lengths (L) of 150 and 300 mm, respectively. Figure 6 shows a cylinder undergoing testing by a universal testing machine with a capacity of 2,000 kN. The splitting tensile strength was calculated using the following formula:

$$fsp = \frac{2P}{\pi \times D \times L}$$

Where:

f_{sp}: Splitting tensile strength (MPa).
P: Applied load in (N).
D: Cylinder diameter (mm).
L: Cylinder length (mm).

3.4 Flexural strength test

To characterize the UHPC modulus of rupture (f_r), prisms with dimensions of 100 mm × 100 mm × 500 mm were prepared according to ASTM C78-22 specification (ASTM, 2010) and tested under two-point loading with a clear span of 450 mm, Figure 7. The following equation is used to determine f_r:

$$f_r = P \times L/b \times h^2$$

Where:

P = maximum applied load in N, L = prism span (450 mm), b = prism width (100 mm), and h: prism depth (100 mm).

TABLE 4 Mix proportions for the 5 UHPC mixes.

Mix code	Cement kg/m^3	SS kg/m^3	SF %	w/c %	SP (%)	Hooked-end Steel fiber	Straight ends Steel fiber	Carbon fiber
M 1	1,000	1,000	25	20	3	1.33%	—	—
M 2	1,000	1,000	25	20	3	—	1.33%	—
M 3	1,000	1,000	25	20	3	1.33%	—	0.2%
M 4	1,000	1,000	25	20	3	—	1.33%	0.2%
M 5	1,000	1,000	25	20	3	0.66%	0.66%	0.2%

SS, Silica Sand; SF, Silica Fume; SP, Superplasticizer; w/c, Water to cement ratio.

TABLE 5 Characterization tests performed on the mixtures.

Mechanical property	Specimen		Testing standard
	Shape	Dimension (mm)	
Compressive strength	Cube	L = 100	BS 1881-1989
Splitting strength	Cylinder	L = 200	ASTM C469-14
		D = 100	
Flexure strength	Prism	L_1 = 500	ASTM C78-22
		L_2 = 100	
		L_3 = 100	
Flow test	—	—	ASTM C1437-20
Modulus of Elasticity	Cylinder	L = 300	ASTM C496-14
		D = 150	

L, length of cube or height of cylinder; D, diameter of cylinder; L_1, length of prism; L_2, width of prism; L_3, height of prism.

FIGURE 2
Cast specimens in cube and cylinder molds.

FIGURE 3
Specimens being cured in wet conditions.

3.5 Modulus of elasticity test

The modulus of elasticity (E_c) is a major parameter affecting the design and analysis of a UHPC member and is typically related to the square root of the compressive strength (f_c') in an empirical relation (Russell et al., 2013). E_c of the examined mixes was characterized experimentally by testing three 150 mm × 300 mm cylinders per mix, each instrumented with 2 strain gages placed within the middle third length of the cylinder in the axial direction (Figure 8). Averaging the two gage readings from all three cylinder tests, E_c for each mix was found using the following equation adopted from the ASTM C469/C479M-14 (ASTM, 2002) standards:

FIGURE 4
A sample of the flow table test.

FIGURE 5
A sample of compressive strength test.

$$E_C = \frac{S_1 - S_2}{\varepsilon_2 - 0.00005}$$

Where:

S_2 = Stress corresponding to 40% of the ultimate capacity, in MPa,

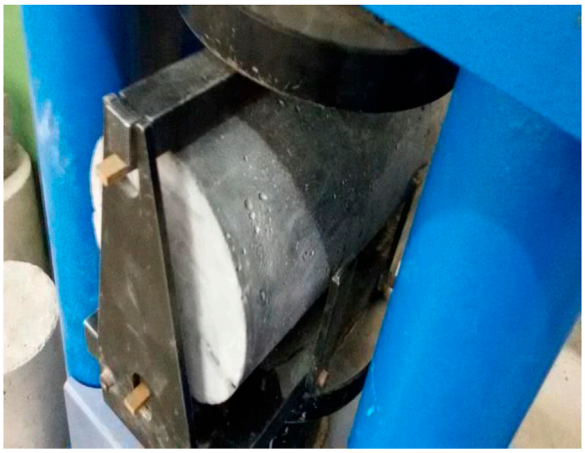

FIGURE 6
A sample of the tensile splitting test.

FIGURE 7
A sample of the flexural strength test.

S_1 = Stress corresponding to a longitudinal strain (ε_1) of 50 millionth,

ε_2 = Longitudinal strain produced by stress S_2.

3.6 Drying shrinkage test

Prismatic 40 mm × 40 mm × 160 mm specimens were used to measure the length change of the concrete sample due to the effects of

FIGURE 8
A sample of modulus of elasticity test.

FIGURE 9
Drying shrinkage test.

drying shrinkage, following specifications of ASTM C157/C157M-14 (Standard, 2014). For each mix, two specimens were tested under room temperature conditions, taking the average of the two as the mix drying shrinkage. A comparator length tool (Figure 9) was used to measure the change in length with time, while the following equation was utilized to determine the shrinkage at any age:

$$\Delta L_x = [(\text{CRD} - \text{initial CRD})/\text{G}] \times 100$$

Where:

ΔL_x = Length change at any age.

CRD = Difference between comparator reading and reference bar at any age.

G = Specimen length.

4 Results and discussion

This section discusses the results of the various material tests conducted to characterize the effects of hybrid fibers on the mechanical performance of UHPC. The results are divided into six sections, each discussing the results of one of the material characterization tests addressed in Section 3.

4.1 Flow table test

The results of the flow table test are presented in Table 6 and Figure 10. The results show a decrease in the flow ability of the UHPC mix, as the fiber percentage increases from 1.33% to 1.53% (15% increase). Previous studies (Boulekbache et al., 2010; Sahoo et al., 2019; Akeed et al., 2022a) have shown that the reduction in flowability associated with the use of fiber reinforcements can be attributed to: 1) the large length and surface area of the fibers compared to the aggregates causing an increase in the cohesive forces between the two constituents; 2) fibers effects on altering the granular skeleton structure of the mix and hindering its flow; 3) fiber reinforcements tend to flow perpendicular to the paste; thus they generate resisting forces and moments to the flow velocity of the fresh mixture (Ahmed H. U. et al., 2022; Abd et al., 2022; Akeed et al., 2022b; Abd et al., 2023).

TABLE 6 Flow table test results.

Mixes type	Flow table test/cm
M 1	21
M 2	23
M 3	19
M 4	20.5
M 5	17

4.2 Compressive strength test

Figure 11 and Table 7 present the results of the compressive strength (f_c') of UHPC for the five different mixes with various fiber blends, at three ages, 7, 28, and 56 days. Comparing mixes 1 and 2, both with 1.33% single-type fibers but featuring type 1 for the former

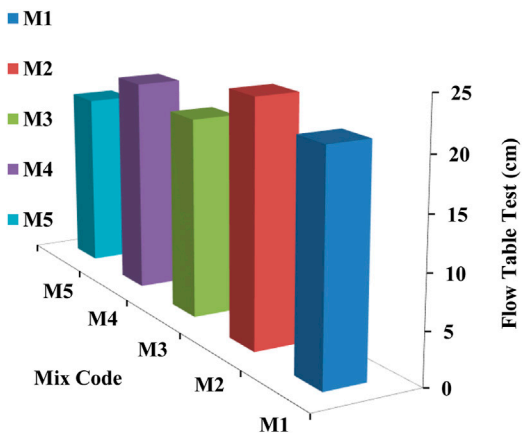

FIGURE 10
Flow measure versus mix-type curves.

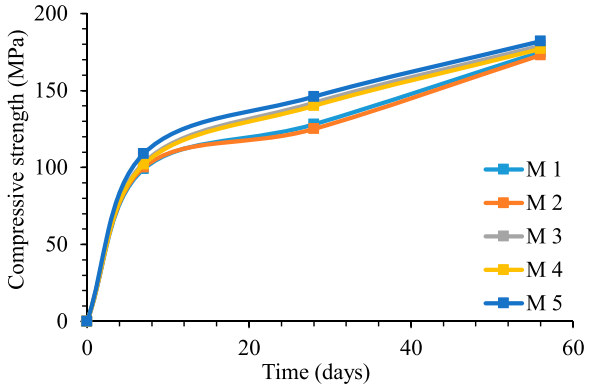

FIGURE 11
Compressive strength versus concrete age curves.

and type 2 for the latter, f_c' seems invariable for all ages (Ali et al., 2022a; El Ouni et al., 2022; Raza et al., 2022). Using a blend of two types of fibers as the case in mixes 3 and 4 seems to result in a negligible increase in $f_c^{'}$ at 7 and 56 days but a noticeable 11.5% increase at 28 days, on average, when compared to f_c' of mixes 1 and 2. On the other hand, the triple fiber type (mix 5) with fiber composition of 0.66% type 1, 0.66% type 2, and 0.2% type 3 results in a 5%–15% increase in $f_c^{'}$ compared to that of the single fiber type mixes (mixes 1 and 2), and 2%–6% compared to the double fiber type mixes (mixes 3 and 4). Incorporating hybrid fibers into the mix optimizes the benefits of each fiber type due to the different material properties for each type as well as different lengths. With microfibers bridging microcracks and macro ones targeting macrocracks, cracks with different sizes can be controlled, eventually improving compressive strength (Aisheh et al., 2022; Ahmed S. N. et al., 2022).

All mixes accrue an increase in f_c' with age, sharply during the first 7 days from casting and at a much slower rate afterwards. Aside from the similarity in trend with conventional concrete and natural hydration process, the presence of parts unique to UHPC, such as superplasticizers and silica fume, also contribute to compressive strength growth with time. For example, silica fume is known to react chemically with calcium hydroxide, thus increasing the strength and reducing the voids inside the concrete (Sahoo et al., 2019; Ahmed et al., 2021; Akeed et al., 2022d; Akeed et al., 2022e).

4.3 Splitting tensile strength test

Although the tensile strength (f_t) of UHPC is higher than that of conventional concrete, it is subpar to the compressive strength. Thus, tensile splitting tests were also performed to examine the effects of hybrid fiber types in improving the tensile strength of UHPC. Table 8 and Figure 12 present the f_t values for the five different mixes at the ages of 7 and 28 days. f_t of mix 2 was 50%–54% larger than that of mix 1, likely because of the larger tensile strength of the straight steel fibers (type 2) compared to the hooked-end ones (type 1). Both mix 1 and 2 contain single-type fibers. Mix 3 with 1.33% type 1 fibers and 0.2% type 3 (total fiver volume = 1.53%) had a 22%–36% larger f_t than mix 1 with 1.33% type 1 fibers. Despite having 13% fewer fibers, mix 2 (with single-type 2 fibers) had f_t 11%–26% larger than that mix 3. Comparing mix 4 and 2, both containing type 2 fibers but a small 0.2% of carbon fibers (type 3) is added to the former, mix 4 had 11% larger f_t. Of the five proportions, mix 5 features the largest f_t, 16.7 MPa at 7 days and 21 MPa at 28 days. This was a 100% increase over mix 1, 32%–35% over mix 2, 50%–67% over mix 3, and 19%–22% over mix 4. In all mixes, f_t increased with age resonating with the trend observed for the tests on compressive strength.

TABLE 7 Results of the compressive strength test.

Mix code	Compressive strength (MPa) at 7-days	Compressive strength (MPa) at 28-days	Compressive strength (MPa) at 56-days
M 1	99	128	175
M 2	100	125	173
M 3	103	142	179
M 4	102	140	177
M 5	109	146	182

TABLE 8 Splitting tensile strength results.

Mix code	Splitting tensile Strength (MPa) at 7-days	Splitting tensile Strength (MPa) at 28-days
M 1	8.2	10.3
M 2	12.6	15.5
M 3	10	14
M 4	14	17.2
M 5	16.7	21

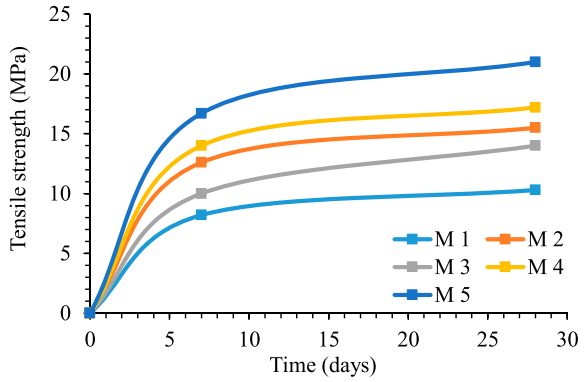

FIGURE 12
Tensile strength versus concrete age curves.

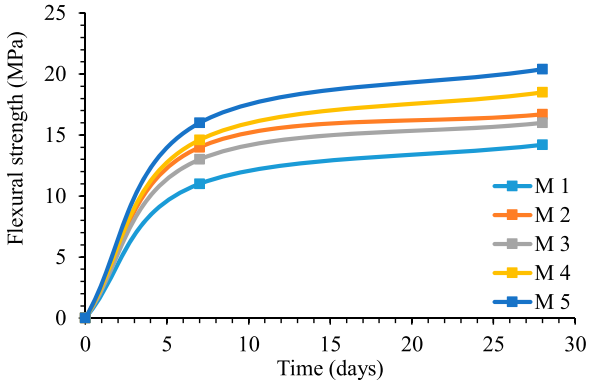

FIGURE 13
Flexural strength versus concrete age curves.

4.4 Flexural strength test

Table 9 and Figure 13 present the results of the effect of using hybrid fibers on the flexural strength (f_b) of UHPC, at the ages of 7 and 28 days. It can be seen that blending carbon fibers (type 3) with hooked-end steel fibers (type 1) as in mix 3 or straight-end steel fibers (type 2) as in mix 4 results in an increase in f_b by about 12.67% and 10.78%, respectively, compared to mix 1 and 2 with single-type fibers. Using the three-type fiber blend resulted in the largest f_b, 20.5 MPa at 28 days. This improvement is due to the increase in the bonding strength between the fibers and the concrete mixture, and thus an increase in the material's ductility. Furthermore, due to the presence of fibers in the mix, higher energy input is required to extend the crack further, and the crack-tip region will be restrained, which can be attributed to the closing pressure on crack surfaces induced by the bridging fibers (Ter Maten, 2011).

4.5 Modulus of elasticity test

Table 10 and Figure 14 present the results of the UHPC elastic modulus (E) for the five mixes, at two ages 7 and 28 days. The results show the hybrid fibres' clear role in increasing the mix's stiffness. When carbon fibers were used with hooked-end steel fibers (mix 3), E increased by about 7.18% compared to mix 1 (type 1 fibers only) and 5.7% compared to mix 2 (type 1 fibers only). Mix 5 (with a blend of all three fiber types) resulted in the highest E 49.63 MPa, at 28 days of age. E of concrete is directly affected by the compressive

TABLE 9 Flexural strength results.

Mix code	Flexural strength (MPa) at 7-days	Flexural strength (MPa) at 28-days
M 1	11	14.2
M 2	14	16.7
M 3	13	16
M 4	14.6	18.5
M 5	16	20.4

TABLE 10 Results for modulus of elasticity test.

Mix code	Modulus of elasticity (GPa) at 7-days	Modulus of elasticity (GPa) at 28-days
M 1	41	44.32
M 2	40.4	43.53
M 3	44.34	47.5
M 4	41.7	46
M 5	46	49.63

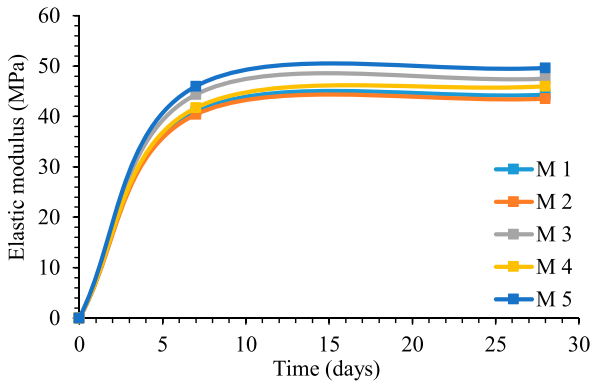

FIGURE 14
Elastic modulus versus concrete age curves.

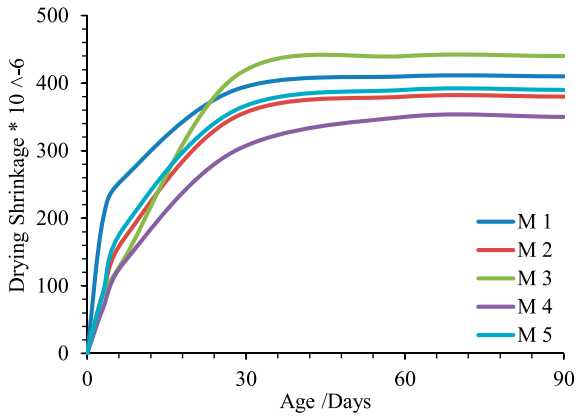

FIGURE 15
Drying shrinkage versus concrete age curves.

strength of concrete (Tomosawa et al., 1990) where fibers have an essential role in reducing the concrete cracking strains due to the crack bridging effects, and ultimately increasing the stiffness.

4.6 Drying shrinkage test

The results of the drying shrinkage test for the five mixes versus age in days are presented in Figure 15. The shrinkage was measured at five ages, namely, 3, 7, 28, 56, and 90 days. In line with other mechanical tests, Figure 15 confirms the advantages of hybrid fibers where mix 5 (with triple fiber type) yielded the smallest values for dry shrinkage.

The functions of the fibers in cement-based composites can be classified into two categories: shrinkage crack control and mechanical property enhancement. For shrinkage crack control, generally lesser amounts of low-modulus and low-strength fibers are added to restrain the early-age shrinkage and suppress shrinkage cracking. Short straight steel fibers can serve as bridging mechanisms during cracking. Therefore, the use of short steel fibers, especially those with a high aspect ratio, is beneficial in that case.

4.7 Discussion on the role of fibers

In conventional applications of fiber cementitious composites, the fibers' function becomes visible after a major crack has formed in the composite (Shah, 1990). At this stage, there are one or few major cracks and the overall composite behaviour is characterized by strain softening after the peak load is reached. The incorporation of fibers significantly increases the total energy consumption and overall toughness of the composite. In such cases, and where fiber rupture does not govern, the gradual fiber debonding and pullout failures can consume a great amount of energy. On the other hand, with an increase in fiber volume fraction, microcracks formed in the matrix may be stabilized due to the interaction between the matrix and fibers through bonding, hence postponing the formation of the first major crack in the matrix. Thus, the apparent tensile strength of the matrix can be increased (Shah, 1990). Moreover, when a sufficient volume fraction of small-diameter steel, glass, or synthetic fibers is incorporated into the cement-based matrix, the fiber/matrix interaction can lead to strain hardening and multiple cracking behaviours, changing the failure mode from quasi-brittle to ductile.

As a result, the composite's toughness and matrix tensile strength can be significantly improved. One of the mechanisms for slowing the growth of a transverse crack in unidirectional fiber composites can be attributed to the development of longitudinal cylindrical shear microcracks located at the boundary between the fiber and the bulk matrix, which allows the fibers to deboned while transferring the force across the faces of the main crack. In addition to enhancing the toughness and tensile strength, the addition of fibers can also improve the bending resistance of cement-based composites. However, adding fibers has only a minor influence on

the compressive strength of cement-based composites. At a small fiber volume fraction, there is almost no effect. Hence, it is not worthwhile to incorporate fibers to enhance compressive strength. The enhancing order of fibers on the mechanical properties of cement-based composites is toughness, followed by flexural strength, tensile strength, and compressive strength (Shah, 1990).

Microfibers are efficient in restraining microcracks and macro fibers in restraining macroscopic cracks. From the materials point of view, the fibers that are commonly used in fiber-reinforced cement-based composites are carbon, glass, polymeric (e.g., acrylic, aramid, nylon, polyester, polyethylene), natural (e.g., wood cellulose, sisal, coir), and steel (high tensile and stainless). Several types of fibers have different values of young's modulus, tensile strength, surface textures, and elongation abilities. These properties affect the bond between the fibers and the matrix, the ability to bridge cracks, the improvement of matrix properties, and, by extension, how fiber-reinforced cement-based composites behave.

5 Conclusion

This study conducted tests on 90 small-scale specimens with different shapes and functions to characterize the effects of blended micro- and macro-size fibers on the mechanical properties of ultra-high performance concrete (UHPC). The fibers studied were hooked-end steel (referred to as type 1, representing macro class), straight-end steel (type 2, intermediate size), and carbon (type 2, micro size). Five mixes were cast and differing by the type and blend of fibers, namely, a) with type 1 unary fibers, b) with type 2 unary fibers, c) with type 1 and 3 binary fiber blend, d) with type 2 and 3 binary fiber blend, and e) with all three fibers. A fiber dosage of 1.56% by volume was used for blended fiber mixes. The characterization tests were performed on the following mechanical properties: flowability, compressive strength, tensile strength, flexural strength, modulus of elasticity, and dry shrinkage. Based on the results, the following conclusions were made:

1. Using ternary fiber cocktail instead of unary type 1 fibers resulted in a 20% decrease in the flowability of the UHPC mix.
2. The compressive strength (f_c'), at ages of 7 and 28 days, does not seem to vary for mixes with unary fibers (type 1 or type 2). f_c' for the mixes with a blend of two types of fibers (type 1 and 3 or type 2 and 3) was slightly larger than that of the unary-fiber mixes at ages of 7 and 56 days, but 11.5% larger at 28 days. The ternary-fiber mix resulted in f_c' of 5%–15% and 2%–6% more than that of the unary-fiber and binary-fiber mixes, respectively.
3. The ternary fiber cocktail improved the UHPC tensile strength by 14% and 16.8%, compared to the mixes featuring unary and binary fibers. This is because of the multiple roles of different fiber classes in bridging various crack sizes.
4. The ternary fiber cocktail resulted in 22.16%–43.66% increase in flexural strength (an indicator of higher ductility) compared to the mixes featuring unary fibers.
5. The modulus of elasticity was increased by 12%–14% when ternary fiber cocktail was used *in lieu* of unary type 1 fibers.
6. The triple-fiber cocktail also resulted in smaller drying shrinkage than the other fiber blends. It is hypothesized that lesser amounts of low-modulus and low-strength fibers results in better restraint of the early-age shrinkage and shrinkage cracking.

Data availability statement

The original contributions presented in the study are included in the article/Supplementary Material, further inquiries can be directed to the corresponding author.

Author contributions

Conception and design of the study: SA, RH, AJ, HN, SM, MB, and MS; acquisition of data: SA, RH, AJ, and HN; analysis and/or interpretation of data: SM, MB, and MS; drafting the manuscript: SA, RH, AJ, HN, SM, MB, and MS; revising the manuscript critically for important intellectual content: SA, RH, AJ, HN, SM, MB, and MS; and approval of the version of the manuscript to be published: SA, RH, AJ, HN, SM, MB, and MS.

Funding

This research was funded by the Ministry of Science and Higher Education of the Russian Federation within the framework of the state assignment No. 075-03-2022-010 dated 14 January 2022 and No. 075-01568-23-04 dated 28 March 2023 (Additional agreement 075-03-2022-010/10 dated 09 November 2022, Additional agreement 075-03-2023-004/4 dated 22 May 2023), FSEG-2022-0010.

Conflict of interest

The authors declare that the research was conducted in the absence of any commercial or financial relationships that could be construed as a potential conflict of interest.

Publisher's note

References

Abd, S. M., Mhaimeed, I. S., Tayeh, B. A., Najm, H. M., and Qaidi, S. (2022). Flamingo technique as an innovative method to improve the shear capacity of reinforced concrete beam. *Case Stud. Constr. Mater.* 17, e01618. doi:10.1016/j.cscm.2022.e01618

Abd, S. M., Mhaimeed, I. S., Tayeh, B. A., Najm, H. M., and Qaidi, S. (2023). Investigation of the use of textile carbon yarns as sustainable shear reinforcement in concrete beams. *Case Stud. Constr. Mater.* 18, e01765. doi:10.1016/j.cscm.2022.e01765

Ahmad, W., Farooq, S. H., Usman, M., Khan, M., Ahmad, A., Aslam, F., et al. (2020). Effect of coconut fiber length and content on properties of high strength concrete. *Materials* 13, 1075. doi:10.3390/ma13051075

Ahmed, B. K., and Abd, S. M. (2018). Eliminating the shrinkage of high strength concrete by using super absorbent polymer (SAP). *Diyala J. Eng. Sci.* 11, 8–13. doi:10.24237/djes.2018.11402

Ahmed, H. U., Mohammed, A. A., Rafiq, S., Mohammed, A. S., Mosavi, A., Sor, N. H., et al. (2021). Compressive strength of sustainable geopolymer concrete composites: A state-of-the-art review. *Sustainability* 13, 13502. doi:10.3390/su132413502

Ahmed, H. U., Mohammed, A. S., Faraj, R. H., Qaidi, S. M. A., and Mohammed, A. A. (2022a). Compressive strength of geopolymer concrete modified with nano-silica: Experimental and modeling investigations. *Case Stud. Constr. Mater.* 16, e01036. doi:10.1016/j.cscm.2022.e01036

Ahmed, S. N., Hamah Sor, N., Ahmed, M. A., and Qaidi, S. M. A. (2022b). Thermal conductivity and hardened behavior of eco-friendly concrete incorporating waste polypropylene as fine aggregate. *Mater. Today Proc.* 57, 818–823. doi:10.1016/j.matpr.2022.02.417

Aisheh, Y. I. A., Atrushi, D. S., Akeed, M. H., Qaidi, S., and Tayeh, B. A. (2022). Influence of steel fibers and microsilica on the mechanical properties of ultra-high-performance geopolymer concrete (UHP-GPC). *Case Stud. Constr. Mater.* 17, e01245. doi:10.1016/j.cscm.2022.e01245

Akeed, M. H., Qaidi, S., Ahmed, H. U., Emad, W., Faraj, R. H., Mohammed, A. S., et al. (2022a). Ultra-high-performance fiber-reinforced concrete. Part III: Fresh and hardened properties. *Case Stud. Constr. Mater.* 17, e01265. doi:10.1016/j.cscm.2022.e01265

Akeed, M. H., Qaidi, S., Ahmed, H. U., Faraj, R. H., Mohammed, A. S., Emad, W., et al. (2022c). Ultra-high-performance fiber-reinforced concrete. Part IV: Durability properties, cost assessment, applications, and challenges. *Case Stud. Constr. Mater.* 17, e01271. doi:10.1016/j.cscm.2022.e01271

Akeed, M. H., Qaidi, S., Ahmed, H. U., Faraj, R. H., Majeed, S. S., Mohammed, A. S., et al. (2022b). Ultra-high-performance fiber-reinforced concrete. Part V: Mixture design, preparation, mixing, casting, and curing. *Case Stud. Constr. Mater.* 17, e01363. doi:10.1016/j.cscm.2022.e01363

Akeed, M. H., Qaidi, S., Ahmed, H. U., Faraj, R. H., Mohammed, A. S., Emad, W., et al. (2022d). Ultra-high-performance fiber-reinforced concrete. Part I: Developments, principles, raw materials. *Case Stud. Constr. Mater.* 17, e01290. doi:10.1016/j.cscm.2022.e01290

Akeed, M. H., Qaidi, S., Ahmed, H. U., Faraj, R. H., Mohammed, A. S., Emad, W., et al. (2022e). Ultra-high-performance fiber-reinforced concrete. Part II: Hydration and microstructure. *Case Stud. Constr. Mater.* 17, e01289. doi:10.1016/j.cscm.2022.e01289

Al-Tayeb, M. M., Aisheh, Y. I. A., Qaidi, S. M. A., and Tayeh, B. A. (2022). Experimental and simulation study on the impact resistance of concrete to replace high amounts of fine aggregate with plastic waste. *Case Stud. Constr. Mater.* 17, e01324. doi:10.1016/j.cscm.2022.e01324

Ali, B., Azab, M., Ahmed, H., Kurda, R., El Ouni, M. H., and Elhag, A. B. (2022a). Investigation of physical, strength, and ductility characteristics of concrete reinforced with banana (Musaceae) stem fiber. *J. Build. Eng.* 61, 105024. doi:10.1016/j.jobe.2022.105024

Ali, B., Farooq, M. A., El Ouni, M. H., Azab, M., and Elhag, A. B. (2022b). The combined effect of coir and superplasticizer on the fresh, mechanical, and long-term durability properties of recycled aggregate concrete. *J. Build. Eng.* 59, 105009. doi:10.1016/j.jobe.2022.105009

Almeshal, I., Al-Tayeb, M. M., Qaidi, S. M. A., Abu Bakar, B. H., and Tayeh, B. A. (2022). Mechanical properties of eco-friendly cements-based glass powder in aggressive medium. *Mater. Today Proc.* 58, 1582–1587. doi:10.1016/j.matpr.2022.03.613

Astm, C. (2010). "Standard test method for flexural strength of concrete (using simple beam with third-point loading)," in American society for testing and materials), 19428–12959.()

Astm, C. (2007). *Standard test method for flow of hydraulic cement mortar*, C1437.

Astm, C. (2002). Standard test method for static modulus of elasticity and Poisson's ratio of concrete in compression. *Annu. book ASTM Stand.* 4, 469.

Biolzi, L., Guerrini, G. L., and Rosati, G. (1997). Overall structural behavior of high strength concrete specimens. *Constr. Build. Mater.* 11, 57–63. doi:10.1016/s0950-0618(96)00026-8

Boulekbache, B., Hamrat, M., Chemrouk, M., and Amziane, S. (2010). Flowability of fibre-reinforced concrete and its effect on the mechanical properties of the material. *Constr. Build. Mater.* 24, 1664–1671. doi:10.1016/j.conbuildmat.2010.02.025

Bs, P. (1989). *Method for determination of compressive strength of concrete cubes*.

Caluk, N., Mantawy, I., and Azizinamini, A. (2019). Durable bridge columns using stay-in-place UHPC shells for accelerated bridge construction. *Infrastructures* 4, 25. doi:10.3390/infrastructures4020025

Cao, M., Li, L., and Khan, M. (2018a). Effect of hybrid fibers, calcium carbonate whisker and coarse sand on mechanical properties of cement-based composites. *Mater. Construcción* 68, e156. doi:10.3989/mc.2018.01717

Cao, M., Xie, C., Li, L., and Khan, M. (2018b). The relationship between reinforcing index and flexural parameters of new hybrid fiber reinforced slab. *Comput. Concr. Int. J.* 22, 481–492.

El Ouni, M. H., Shah, S. H. A., Ali, A., Muhammad, S., Mahmood, M. S., Ali, B., et al. (2022). Mechanical performance, water and chloride permeability of hybrid steel-polypropylene fiber-reinforced recycled aggregate concrete. *Case Stud. Constr. Mater.* 16, e00831. doi:10.1016/j.cscm.2021.e00831

Emad, W., Mohammed, A. S., Bras, A., Asteris, P. G., Kurda, R., Muhammed, Z., et al. (2022). Metamodel techniques to estimate the compressive strength of UHPFRC using various mix proportions and a high range of curing temperatures. *Constr. Build. Mater.* 349, 128737. doi:10.1016/j.conbuildmat.2022.128737

Faraj, R. H., Ahmed, H. U., Rafiq, S., Sor, N. H., Ibrahim, D. F., and Qaidi, S. M. A. (2022). Performance of self-compacting mortars modified with nanoparticles: A systematic review and modeling. *Clean. Mater.* 4, 100086. doi:10.1016/j.clema.2022.100086

Gao, X. (2007). *Mix design and impact response of fibre reinforced and plain reactive powder concrete*. RMIT University.

Graybeal, B. (2014). *Design and construction of field-cast UHPC connections*. Washington, DC: United States. Federal Highway Administration.

Grünewald, S. (2004). *Performance-based design of self-compacting fibre reinforced concrete*.

Harris, D. K., and Roberts-Wollmann, C. L. (2005). *Characterization of the punching shear capacity of thin ultra-high performance concrete slabs*. Charlottesville, VA: Virginia Center for Transportation Innovation and Research.

He, X., Yuhua, Z., Qaidi, S., Isleem, H. F., Zaid, O., Althoey, F., et al. (2022). Mine tailings-based geopolymers: A comprehensive review. *Ceram. Int.* 48, 24192–24212. doi:10.1016/j.ceramint.2022.05.345

Khan, M., Cao, M., Chu, S., and Ali, M. (2022). Properties of hybrid steel-basalt fiber reinforced concrete exposed to different surrounding conditions. *Constr. Build. Mater.* 322, 126340. doi:10.1016/j.conbuildmat.2022.126340

Khan, M., Cao, M., Hussain, A., and Chu, S. H. (2021). Effect of silica-fume content on performance of CaCO3 whisker and basalt fiber at matrix interface in cement-based composites. *Constr. Build. Mater.* 300, 124046. doi:10.1016/j.conbuildmat.2021.124046

Khan, U. A., Jahanzaib, H. M., Khan, M., and Ali, M. (2018). "Improving the tensile energy absorption of high strength natural fiber reinforced concrete with fly-ash for bridge girders," in *Key engineering materials* (Switzerland: Trans Tech Publ), 335–342.

Puzatova, A., Shakor, P., Laghi, V., and Dmitrieva, M. (2022). Large-scale 3D printing for construction application by means of robotic arm and gantry 3D printer: A review. *Buildings* 12, 2023. doi:10.3390/buildings12112023

Qaidi, S. M. A., Dinkha, Y. Z., Haido, J. H., Ali, M. H., and Tayeh, B. A. (2021a). Engineering properties of sustainable green concrete incorporating eco-friendly aggregate of crumb rubber: A review. *J. Clean. Prod.* 324, 129251. doi:10.1016/j.jclepro.2021.129251

Qaidi, S. M. A., Tayeh, B. A., Zeyad, A. M., De Azevedo, A. R. G., Ahmed, H. U., and Emad, W. (2022a). Recycling of mine tailings for the geopolymers production: A systematic review. *Case Stud. Constr. Mater.* 16, e00933. doi:10.1016/j.cscm.2022.e00933

Qaidi, S. M., Atrushi, D. S., Mohammed, A. S., Ahmed, H. U., Faraj, R. H., Emad, W., et al. (2022b). Ultra-high-performance geopolymer concrete: A review. *Constr. Build. Mater.* 346, 128495. doi:10.1016/j.conbuildmat.2022.128495

Qaidi, S., Yahia, A., Tayeh, B. A., Unis, H., Faraj, R., and Mohammed, A. (2022c). 3D printed geopolymer composites: A review. *Mater. Today Sustain.* 20, 100240. doi:10.1016/j.mtsust.2022.100240

Qaidi, S. M. A., Sulaiman Atrushi, D., Mohammed, A. S., Unis Ahmed, H., Faraj, R. H., Emad, W., et al. (2022d). Ultra-high-performance geopolymer concrete: A review. *Constr. Build. Mater.* 346, 128495. doi:10.1016/j.conbuildmat.2022.128495

Qaidi, S. M. A., Tayeh, B. A., Ahmed, H. U., and Emad, W. (2022e). A review of the sustainable utilisation of red mud and fly ash for the production of geopolymer composites. *Constr. Build. Mater.* 350, 128892. doi:10.1016/j.conbuildmat.2022.128892

Qaidi, S. M. A., Tayeh, B. A., Isleem, H. F., De Azevedo, A. R. G., Ahmed, H. U., and Emad, W. (2022f). Sustainable utilization of red mud waste (bauxite residue) and slag for the production of geopolymer composites: A review. *Case Stud. Constr. Mater.* 16, e00994. doi:10.1016/j.cscm.2022.e00994

Raza, S. S., Ali, B., Noman, M., Fahad, M., and Elhadi, K. M. (2022). Mechanical properties, flexural behavior, and chloride permeability of high-performance steel fiber-reinforced concrete (SFRC) modified with rice husk ash and micro-silica. *Constr. Build. Mater.* 359, 129520. doi:10.1016/j.conbuildmat.2022.129520

Raza, S. S., Qureshi, L. A., Ali, B., Raza, A., and Khan, M. M. (2021). Effect of different fibers (steel fibers, glass fibers, and carbon fibers) on mechanical properties of reactive powder concrete. *Struct. Concr.* 22, 334–346. doi:10.1002/suco.201900439

Rossi, P., Acker, P., and Malier, Y. (1987). Effect of steel fibres at two different stages: The material and the structure. *Mater. Struct.* 20, 436–439. doi:10.1007/bf02472494

Russell, H. G., Graybeal, B. A., and Russell, H. G. (2013). *Ultra-high performance concrete: A state-of-the-art report for the bridge community". United states*. McLean, Virginia: Federal Highway Administration. Office of Infrastructure.

Saeed, A., Najm, H. M., Hassan, A., Sabri, M. M. S., Qaidi, S., Mashaan, N. S., et al. (2022). Properties and applications of geopolymer composites: A review study of mechanical and microstructural properties. *Materials* 15, 8250. doi:10.3390/ma15228250

Sahoo, K. K., Sarkar, P., and Davis, R. (2019). Mechanical properties of silica fume concrete designed as per construction practice. *Proc. Institution Civ. Engineers-Construction Mater.* 172, 20–28. doi:10.1680/jcoma.16.00085

Sanjuán, M. Á., and Andrade, C. (2021). Reactive powder concrete: Durability and applications. *Appl. Sci.* 11, 5629. doi:10.3390/app11125629

Shah, S. P. (1990). *Toughening of cement-based materials with fiber reinforcement*, MRS Online Proceedings Library (OPL. 211.

Shaheen, E., and Shrive, N. G. (2006). Optimization of mechanical properties and durability of reactive powder concrete. *ACI Mater. J.* 103, 444.

Shakor, P., Nejadi, S., Paul, G., and Malek, S. (2019a). Review of emerging additive manufacturing technologies in 3D printing of cementitious materials in the construction industry. *Front. Built Environ.* 4, 85. doi:10.3389/fbuil.2018.00085

Shakor, P., Nejadi, S., Paul, G., Sanjayan, J., and Nazari, A. (2019b). Mechanical properties of cement-based materials and effect of elevated temperature on three-dimensional (3-D) printed mortar specimens in inkjet 3-D printing. *ACI Mater. J.* 116, 55–67.

Standard, A. (2014). *C157,"Standard test method for length change of hardened hydraulic-cement mortar and concrete"*. West Conshohocken, PA, United States: Annual Book of ASTM Standards. 4.

Standard, A. (2017). *C496/C496M-17 Standard test method for splitting tensile strength of cylindrical concrete specimens*. West Conshohocken PA: ASTM International.

Tayeh, B. A., Akeed, M. H., Qaidi, S., and Bakar, B. H. A. (2022a). Influence of microsilica and polypropylene fibers on the fresh and mechanical properties of ultra-high performance geopolymer concrete (UHP-GPC). *Case Stud. Constr. Mater.* 17, e01367. doi:10.1016/j.cscm.2022.e01367

Tayeh, B. A., Akeed, M. H., Qaidi, S., and Bakar, B. H. A. (2022b). Influence of sand grain size distribution and supplementary cementitious materials on the compressive strength of ultrahigh-performance concrete. *Case Stud. Constr. Mater.* 17, e01495. doi:10.1016/j.cscm.2022.e01495

Tayeh, B. A., Akeed, M. H., Qaidi, S., and Bakar, B. H. A. (2022c). Influence of the proportion of materials on the rheology and mechanical strength of ultrahigh-performance concrete. *Case Stud. Constr. Mater.* 17, e01433. doi:10.1016/j.cscm.2022.e01433

Tayeh, B. A., Akeed, M. H., Qaidi, S., and Bakar, B. H. A. (2022d). Ultra-high-performance concrete: Impacts of steel fibre shape and content on flowability, compressive strength and modulus of rupture. *Case Stud. Constr. Mater.* 17, e01615. doi:10.1016/j.cscm.2022.e01615

Ter Maten, R. (2011). *Ultra high performance concrete in large span shell structures*.

Tomosawa, F., Noguchi, T., and Onoyama, K. (1990). "Investigation of fundamental mechanical properties of high-strength concrete," in *Summaries of technical papers of annual meeting of* Architectural Institute of Japan*)*, 497–498.()

Vinod, S., Shakor, P., Sartipi, F., and Karakouzian, M. (2022). Object detection using ESP32 cameras for quality control of steel components in manufacturing structures. *Arabian J. Sci. Eng.*, 1–18. doi:10.1007/s13369-022-07562-2

Zeybek, Ö., Özkılıç, Y. O., Karalar, M., Çelik, A. İ., Qaidi, S., Ahmad, J., et al. (2022). Influence of replacing cement with waste glass on mechanical properties of concrete. *Materials* 15, 7513. doi:10.3390/ma15217513